Optimal Readout Schemes in SPAD-Based Time-Correlated Event Detection Sensor for Quantum Imaging Applications

Majid Zarghami, Leonardo Gasparini, and David Stoppa
Fondazione Bruno Kessler
Trento, Italy
Email: zarghami@fbk.eu

***Abstract*—CMOS SPAD imagers are potentially good candidates for detection of entangled photons in Quantum Imaging applications thanks to their sub-nanosecond time-resolved capabilities and highly parallel readout. In this context, the low number of photons that are typically detected corresponds to a very sparse data matrix. A full readout of raw data is therefore a waste of time and power. We have implemented a sensor architecture to improve the efficiency of the observation up to 8.46% in a TDC-based pixel structure. A tunable current source is used per pixel to establish a global current. This global current presents a real-time status of the whole pixel array in terms of triggered SPADs. The proposed solution requires minimal extra pixel electronics, with little impact on the fill factor and allows an observation rate of up to 8.5 Mfps.**

I. Introduction

Quantum imaging exploits the properties of quantum optical states to go beyond the limits of classical imaging. It often relies on entangled photons, exploiting their strong correlations to predict the interaction of light with matter. Entangled photon states are instantaneously generated by a source, and therefore, the time coincidence characteristic of entangled photons has an important role in this imaging method [1]. However, this coincidence is accompanied with uncertainty which is referred to the random optical and electrical time delays in the system. For example, photon flux is a stochastic process, and the photodetector module has a finite electronic timing jitter. As the degree of entanglement is typically limited to few photons, mostly pairs, a detector with time-resolved single-photon detection capabilities is needed to detect the coincident photons. The main goal of the current work is to achieve a global macro time gating in the order of 10ns to filter out the most of uncorrelated photons, combined with a fine coincidence detection in the order of 100ps, which is a typical requirement for entangled photon detection, while keeping a large duty cycle.

A recent development in single photon detection are SPAD imagers implemented in standard CMOS technology. CMOS SPAD arrays combine high spatial resolution, typical of standard CMOS imagers, with the deep sub-nanosecond temporally resolving capabilities of Photo-Multiplier Tubes (PMT) and Silicon Photo-Multipliers (SiPM). Competing technologies such as the Electron-Multiplying CCD (EMCCD) show drawbacks like costly cooling and relatively large gating time window (in the order of tens of nanoseconds). Therefore, CMOS SPAD arrays represent a valid alternative to them [1]. Coincidence detection in a CMOS SPAD array is achieved by using time-gating or photon timestamping. Time gating consists in enabling the detection of photons in a very short time window [2], synchronously with respect to a global signal (e.g., a clock or a trigger generated by a pulsed laser). This method is particularly effective in fully synchronous setups, when the exact photon arrival time is known. [1] presents a state-of-the-art review of time-gated approaches which are as short as few hundreds of picoseconds. This method needs a synchronous format of entangled photons but typically there is no time information available on the source generating the photons. There is therefore no possibility to utilize the time gating method in the current application. Photon timestamping is achieved using time converters to either analog or digital. Time converters provide an output proportional to the arrival time of the photon. Time-to-Analog Converters (TAC) suggest good performances in terms of compactness and low power consumption [3]. However, their non-uniformity and low frame rate have to be taken into account. Time-to-Digital Converters (TDC), in spite of having large area and power consumption characteristics, achieve greater robustness and higher frame rates [4][5]. We implemented a kilopixel quantum image sensor with per-pixel TDC, supporting an observation window in the order of 10ns, while the full readout process takes about $10.56\mu s$.

Typically, all the pixels in the array in a TAC and TDC-based architecture are read out even if there are no detected photons or even if most of the data is zero (i.e., no photons detected). In a quantum optics experiment that aimed at analyzing the statistics of N^{th} order photon states, with N = 2, 3, 4, 5, most of the frames are empty [1]. Moreover, the probability of generating and detecting N entangled photons decreases exponentially with N. In [1], a total of 3.07M events were recorded. Since each scan of the whole array takes $10.56\mu s$ and considering a 1% probability of 5-fold coincidence photons, the measurement time using our detector would have been 54 minutes.

This work presents an architectural solution to improve the acquisition efficiency of the SPAD-based detector. It consists a method to evaluate the number of pixels fired within the

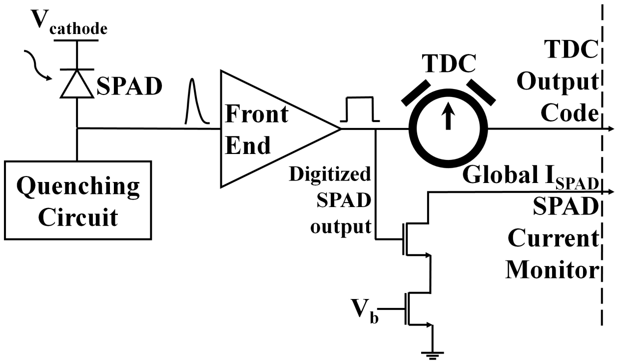

Fig. 1. One-pixel block diagram.

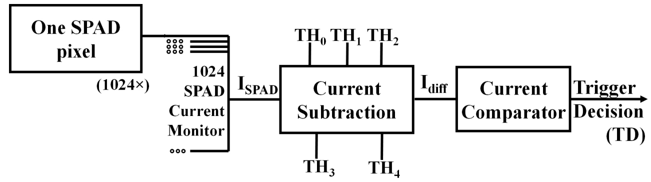

Fig. 2. Trigger decision block diagram.

previous observation window and it can be used to skip the readout of the current frame and acquire a new one. This solution, combined with a readout method that entirely skips a whole row if no pixel is fired during the observation time, would reduce the acquisition time down to 36 seconds. These methods are independent of the coincidence detection method. In fact, the first method enables to read out when the frame has enough photons, and the second one is proposed to speed up scanning.

The following section of this paper describes the proposed solution to readout a frame in a smart way to achieve high observation rate. In section III we describe the monitoring operation of pixel array in detail and section IV provides the simulation result of this strategy. Our conclusions are outlined in Section V.

II. Activity Monitor Architecture

The proposed solution aims at understanding if a predefined minimum number of photons have been detected in the last observation window. The circuit should be as fast as possible in order to minimize the dead times; possibly it should take much less time than the laser period (in case a pulsed source is used), so that we have enough time to reset the sensor and start the new acquisition in correspondence with the next laser pulse.

A current-based approach is considered in Fig. 1, showing the block diagram of a TDC-based pixel. Each pixel draws a fixed amount of current from a global net only if it fired. Individual pixel contributions sum up at global level, and the resulting current is compared with a threshold. In case, a trigger is generated to start the readout process. Otherwise the frame is skipped. Each pixel contains a SPAD detector, quenching circuit and the front-end. The other block is a TDC, transforming the photon arrival time to a digital code. There are two other transistors which represent the key feature of our implementation and operate as a tunable current source. As it can be seen in Fig. 1, the I_{SPAD} current is enabled by the digitized and latched SPAD output signal and sinks from a global net. Hence, the current flowing denotes one photon detection and is referred to as SPAD Monitor = I_{SPAD}.

Fig. 2 shows the block diagram of the proposed sensor. It consists of a 1024-pixel array, generating 1024 current paths sourcing from a single, global path. The I_{SPAD} is therefore proportional to the number of triggered SPADs. There are two blocks to recognize the number of triggered SPADs. The first block is a current subtractor. This block receives as inputs a five-bit threshold and I_{SPAD}. The threshold, expressed in decimal form, represents the maximum number of detected photons to skip the readout of the acquired frame. A current proportional to the threshold is generated and subtracted from the input current. The resulting current I_{diff} is then sent to a current comparator, which evaluates if I_{diff} is greater than zero and in case generates the signal that triggers the readout process. The following section describes the current subtraction and comparator circuit operation in more detail.

The current subtractor schematic is presented in Fig. 3. There are two branches, left and right. The right branch builds up the threshold current, according to the user-defined input configuration. The current corresponding to 1 LSB of the threshold is matched with the I_{SPAD} generated in a pixel. The current source that sinks half of the photon current, is to avoid comparing two equal currents. The total threshold current is mirrored on the left arm.

M_{bL} and M_{bR} are transistors having same size and bias

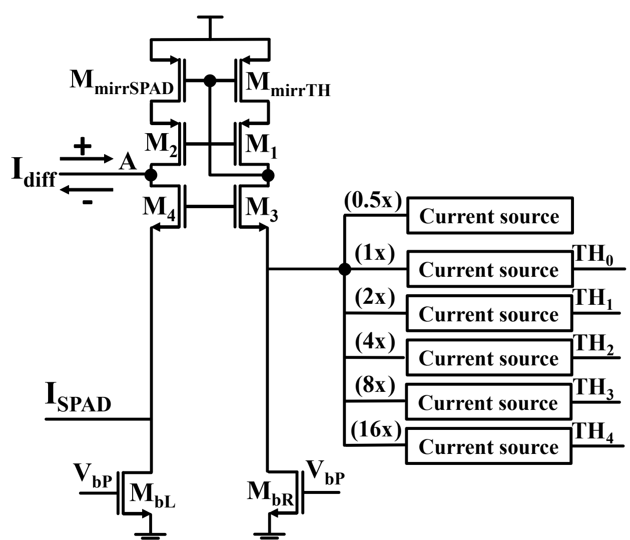

Fig. 3. Current subtraction schematic.

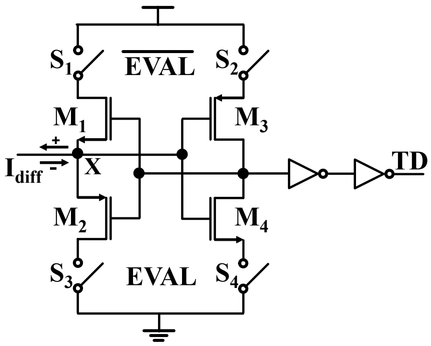

Fig. 4. Current comparator schematic.

voltage, therefore their current is identical. In the right part of the schematic, there are 5 current sources. Each one includes an increasing number of elementary current generators, and is controlled by one of the 5 threshold bits. TH_0, TH_1, TH_2, TH_3, TH_4 represent one, two, four, eight and sixteen SPAD current quantities, respectively. In the left side of the mirror, the mirrored threshold current is subtracted from the I_{SPAD}, generating the difference current I_{diff}, which is then fed to the current comparator. In each evaluation time, based on I_{SPAD} magnitude and the given threshold, there are two possible outcomes from this block. If the number of triggered SPAD is lower or equal to the threshold value, I_{diff} is negative. If the triggered SPAD is more than the threshold, I_{diff} is positive.

A modified version of the current comparator presented in [6] is used in order to detect the sign of I_{diff}. The schematic of the implemented current comparator is presented in Fig. 4. Switching transistors S_1, S_2, S_3, S_4 are added to activate the comparator only at the end of the observation window for a short evaluation time by means of the EVAL signal. When I_{diff} is negative, M_2 is ON and therefore TD is zero. On the other hand, When I_{diff} is positive, M_1 is ON and therefore TD is in its high level and it provides a meaningful information; this situation happens when the detected photons are more than the minimum required number of photons.

III. Simulation Results

Fig. 5 illustrates the simulation results about the operations of current subtraction and current comparison. A threshold level corresponding to 5 triggered SPADs have been used. Here, each photon/threshold LSB contributes to the global current adding 8.92μA. Its intensity can be adjusted by changing a reference voltage V_b (Fig. 1). The simulation shows three consecutive observations, in which 4, 5 and 6 photons were detected respectively. Hence, in the first and second events the number of activated SPAD is lower or equal to the threshold quantity, while in the third case the threshold is exceeded and TD is correctly set high.

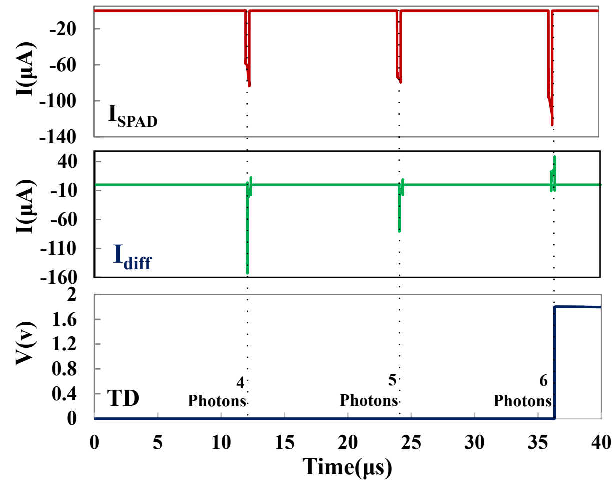

Fig. 5. Impact of different number of photon on TD.

The intestity of I_{SPAD} affects the TD activation time. In Fig. 6 two values are considered for I_{SPAD}. The simulations indicate that the larger current difference results in a faster comparison. This has to be attributed to the non-negligible parasitic capacitance at node X, which is the limiting factor for this current comparator architecture. The graph also shows that one can boost the comparators speed by adjusting V_b in the current generators, at the expense of a larger power consumption.

IV. Conclusion

In this paper, a novel readout scheme with high time performance for SPAD-based quantum imager has been described. The proposed strategy utilizes two more transistors per pixel, having a limited impact on the pixel fill factor. They convert the digital output from the SPAD front-end into a current, which is summed across the whole array. The total current in turn determines the number of stimulated SPADs in real time. A decision block receives this global current as an input and makes a notification of occurrence of at least N photon coincidence, where N is programmable in the 0-31 range. If no trigger is generated by the decision block, the frame is

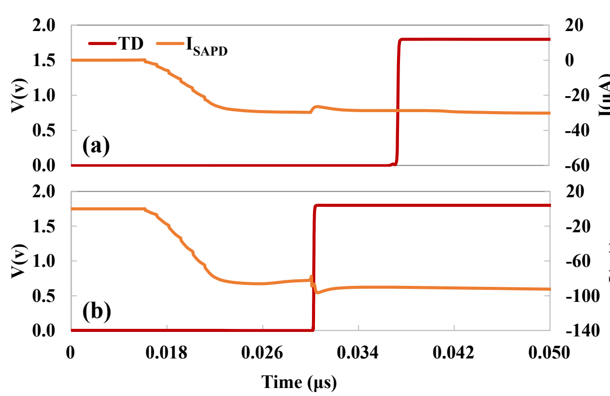

Fig. 6. Current subtraction schematic.

skipped and a new acquisition is run, without losing time in reading out the meaningless data. Otherwise, the whole array is scanned one row at a time for readout. This mechanism, along with the possibility of skipping empty rows during readout, leads to a reduction in readout time by a factor of 5.5 and a duty cycle improvement from 0.095% to 8.46%. Considering the experiment in [1], the measurement time reduces from 54 minutes to 36 seconds.

REFERENCES

[1] M. Unternährer, B. Bessire, L. Gasparini, D. Stoppa, and A. Stefanov, "Coincidence detection of spatially correlated photon pairs with a monolithic time-resolving detector array," *Optics Express*, vol. 24, no. 25, pp. 28 829–28 841, 2016.

[2] M. Perenzoni, L. Pancheri, and D. Stoppa, "Compact SPAD-based pixel architectures for time-resolved image sensors," *Sensors*, vol. 16, no. 5, p. 745, 2016.

[3] N. A. Dutton, I. Gyongy, L. Parmesan, S. Gnecchi, N. Calder, B. R. Rae, S. Pellegrini, L. A. Grant, and R. K. Henderson, "A SPAD-based QVGA image sensor for single-photon counting and quanta imaging," *IEEE Transactions on Electron Devices*, vol. 63, no. 1, pp. 189–196, 2016.

[4] S. Jahromi, J.-P. Jansson, and J. Kostamovaara, "Solid-state 3D imaging using a 1nJ/100ps laser diode transmitter and a single photon receiver matrix," *Optics Express*, vol. 24, no. 19, pp. 21 619–21 632, 2016.

[5] M. Perenzoni, D. Perenzoni, and D. Stoppa, "A 64 x 64-pixels digital silicon photomultiplier direct TOF sensor with 100-Mphotons/s/pixel background rejection and imaging/altimeter mode with 0.14% precision up to 6 km for spacecraft navigation and landing," *IEEE Journal of Solid-State Circuits*, vol. 52, no. 1, pp. 151–160, 2016.

[6] H. Traff, "Novel approach to high speed CMOS current comparators," *Electronics Letters*, vol. 28, no. 3, pp. 310–312, 1992.